Hindawi Publishing Corporation
Oxidative Medicine and Cellular Longevity
Volume 2016, Article ID 9460462, 18 pages
http://dx.doi.org/10.1155/2016/9460462

*Research Article*

# The Protective Roles of ROS-Mediated Mitophagy on $^{125}$I Seeds Radiation Induced Cell Death in HCT116 Cells

**Lelin Hu,[1,2] Hao Wang,[1] Li Huang,[1] Yong Zhao,[3] and Junjie Wang[1]**

[1]*Department of Radiation Oncology, Peking University 3rd Hospital, Haidian District, Beijing 100191, China*
[2]*School of Medicine, Anhui University of Science and Technology, Huainan 232001, Anhui, China*
[3]*State Key Laboratory of Membrane Biology, Institute of Zoology, Chinese Academy of Sciences, Beijing 100101, China*

Correspondence should be addressed to Junjie Wang; junjiewangedu@163.com

Received 17 September 2016; Revised 18 November 2016; Accepted 24 November 2016

Academic Editor: Sander Bekeschus



For many unresectable carcinomas and locally recurrent cancers (LRC), $^{125}$I seeds brachytherapy is a feasible, effective, and safe treatment. Several studies have shown that $^{125}$I seeds radiation exerts anticancer activity by triggering DNA damage. However, recent evidence shows mitochondrial quality to be another crucial determinant of cell fate, with mitophagy playing a central role in this control mechanism. Herein, we found that $^{125}$I seeds irradiation injured mitochondria, leading to significantly elevated mitochondrial and intracellular ROS (reactive oxygen species) levels in HCT116 cells. The accumulation of mitochondrial ROS increased the expression of HIF-1$\alpha$ and its target genes BINP3 and NIX (BINP3L), which subsequently triggered mitophagy. Importantly, $^{125}$I seeds radiation induced mitophagy promoted cells survival and protected HCT116 cells from apoptosis. These results collectively indicated that $^{125}$I seeds radiation triggered mitophagy by upregulating the level of ROS to promote cellular homeostasis and survival. The present study uncovered the critical role of mitophagy in modulating the sensitivity of tumor cells to radiation therapy and suggested that chemotherapy targeting on mitophagy might improve the efficiency of $^{125}$I seeds radiation treatment, which might be of clinical significance in tumor therapy.

## 1. Introduction

Due to its low complication rates and high efficacy—which is comparable to that of radical surgery and external beam radiation therapy—$^{125}$I seeds implantation brachytherapy has become one of the most popular treatment modalities for many unresectable carcinomas and locally recurrent cancers [1–7]. A series of studies have explored the molecular mechanisms through which $^{125}$I seeds radiation exerts anticancer activity. Most studies have focused on apoptosis and cell cycle arrest resulting from DNA damage after exposure to $^{125}$I seeds radiation [8–10]. However, there is growing evidence that mitochondria, which account for up to 30% of the total cell volume, may also be important extranuclear mediators of the cytotoxic effects of radiation [11, 12]. Healthy mitochondria act as powerhouses, producing energy for cell function through the TCA cycle (tricarboxylic acid cycle) and oxidative phosphorylation [13]. Damage to mitochondria can lead to cell death and a variety of other problems [14].

Mitophagy, which refers to the selective removal of damaged or unwanted mitochondria, is crucial for mitochondrial quality control following stresses such as starvation, photo damage, hypoxia, and ROS production [15]. Certain physiological stresses can induce mitochondrial damage, which can cause oxidative stress and cell death triggered by the production of ROS from the mitochondrial electron transport chain (ETC). The high level of ROS can be selectively sequestered in autophagosomes and subjected to lysosomal degradation in a process termed mitophagy to promote cellular homeostasis and survival [16]. Mitophagy can thus alleviate cell injury following stress, acting as an effective antioxidant pathway and clearing increased mitochondrial or cytosolic ROS. Mitophagy has been reported to be involved in tumor resistance to therapy by maintaining healthy mitochondria [17, 18].

Mitophagy is mediated by specific receptors such as NIX, BNIP3, and FUNDC1 in mammalian systems [19]. BNIP3 and NIX are two important mitochondrial stressor sensors with homology to BCL2 in the BH3 domain. Once

mitophagy is triggered, BNIP3 and NIX are selectively recruited to dysfunctional mitochondria and then bound to the conserved LC3-interacting region (LIR) of LC3-II present on autophagosome to promote removal of damaged mitochondria by the autophagosome [16, 20, 21]. In addition, both BNIP3 and NIX facilitate mitophagy by promoting the release of Beclin1 from the Beclin1-Bcl2/Bcl-X complex [22]. NIX and BNIP3, two hypoxia-inducible proteins that target mitochondria for autophagosomal degradation, are the transcription products of HIF-1$\alpha$ [23]. HIF-1$\alpha$ is an important predictor of tumor progression for several types of solid cancers and can regulate the transcription of a number of genes (such as *BNIP3* and *NIX*) that are involved in mitophagy and apoptosis [24]. Several studies have shown that elevated mitochondrial ROS increases the expression of HIF-1$\alpha$ and its target genes BNIP3/NIX [17, 25].

In the present study, we have focused on the regulatory roles of autophagy in the radiosensitivity of tumors to $^{125}$I seeds irradiation as well as the molecular mechanisms that underlie $^{125}$I seeds radiation induced mitophagy. We found that mitophagy significantly decreased the sensitivity of tumor cells to $^{125}$I seeds irradiation. Thus, targeting mitophagy combined with radiotherapy may improve the therapeutic efficiency in clinical patients with tumors, which needs to be confirmed by the clinical studies.

## 2. Materials and Methods

*2.1. $^{125}$I Radiation Source.* The $^{125}$I seeds used as the radiation source in this study were purchased from Ningbo Junan Pharmaceutical Technology Company (Ningbo, Zhe Jiang province, China) and were installed in an in-house model developed in our laboratory for in vitro $^{125}$I seeds radiation. A detailed description of this model has been published earlier [26, 27]. $^{125}$I seeds have a half-life of ~59.4 days. The experimentally applicable radiation dose rate of $^{125}$I seeds ranged from 2.77 cGy/h to 1.385 cGy/h, which is approximate to the clinically applicable radiation dose rate used in permanent LRC brachytherapy. This model was validated by using thermoluminescent dosimetry (TLD) measurement, and the irradiation time was calculated according to the absorbed dose and initial radiation dose rate. The control cells were seeded and harvested at the same time points as the irradiated cells.

*2.2. Reagents and Antibodies.* Annexin V-FITC apoptosis detection kit I was purchased from Beijing Zoman Biotechnology (Beijing, China); the ROS assay kit and mitochondrial membrane potential assay kit with JC-1 were purchased from Beyotime (Shanghai, China); the mitochondrial ROS indicator MitoSOX was purchased from Invitrogen (Carlsbad, CA, USA); N-acetylcysteine (NAC) and chloroquine (CQ) were purchased from Sigma-Aldrich; 3-methyladenine (3-MA) was purchased from Selleck Chemicals LLC (Houston, TX, USA); Ly294002 was purchased from Invitrogen; Antimycin A was purchased from Sigma-Aldrich. LipofectamineTM 2000 was purchased from Invitrogen. Diphenyleneiodonium chloride (DPI) was purchased from Gene Operation Co., Ltd. (Wuxi, China). cDNA reverse transcription kit and real-time PCR kit were purchased from Takara Biotechnology (Dalian, China); and goat anti-rabbit IgG-horseradish peroxidase (HRP), goat anti-mouse IgG-HRP, anti-$\beta$-actin, and anti-LC3 polyclonal antibody were obtained from Sigma-Aldrich.

*2.3. Cell Culture.* Human colorectal cancer cells—HCT116 cells—were kindly provided by Dr. Xiaojuan Du of Peking University Health Science Center, Beijing, China. The HCT116 cells were grown in RPMI (Roswell Park Memorial Institute) 1640 medium supplemented with 10% fetal calf serum (FCS), 100 units/mL penicillin, and 100 $\mu$g/mL streptomycin, in a humidified atmosphere containing 5% $CO_2$ at 37°C.

*2.4. Clonogenic Survival Assay.* HCT116 cells in appropriate numbers were seeded in 35 mm dishes to ensure the formation of about 100 colonies per dish. After 24 hours, the cells were exposed to $^{125}$I seeds irradiation in the model. At the desired time points, the cells were removed from the radiation source and cultured for 10–12 days [28]. They were then fixed with absolute ethanol and glacial acetic acid in a 1 : 1 ratio at 4°C for 30 minutes and stained with methylene blue for 2 hours. Finally, the samples were washed with cold phosphate-buffered saline (PBS) and dried at room temperature. The number of colonies per dish was counted and the survival fraction (SF) was calculated as PE (tested group)/PE (0-Gy group), where PE was (colony number/number of inoculating cells) × 100%. The experiment was repeated two times in duplicate. The survival fraction values were presented as the mean ± SD for the respective radiation doses.

*2.5. Western Blot Analysis.* Cells were lysed in a radio immunoprecipitation assay (RIPA) buffer (50 mM of pH-7.4 Tris-HCl, 1% NP-40, 0.25% Na-deoxycholate, 150 mM NaCl, and 1 mM of pH-7.4 EDTA) with protease and phosphatase inhibitor cocktails for 15 minutes on ice and then centrifuged for 30 minutes at 12,000$g$ and 4°C. Bicinchoninic acid (BCA) protein assay kits (Beyotime Biotech, Shanghai, China) were used to measure the protein concentrations of protein supernatant. Equal amounts of the protein samples were denatured at 95°C for 5 minutes and then separated on dodecyl sulfate-polyacrylamide gel electrophoresis (SDS-PAGE) gel. Proteins were transferred onto polyvinylidene difluoride (PVDF) membranes (Hybond-P; Amersham, Buckinghamshire, UK) for 2 hours at 100 V on ice. Membranes were blocked with 5% nonfat milk in Tris-buffered saline and Tween 20 (TBST) for 1 hour at room temperature and then incubated overnight at 4°C with the indicated primary antibody. After washing thrice with TBST, the membranes were blotted with the respective secondary antibody for 1 hour at room temperature. The membranes were incubated with enhanced chemiluminescence (ECL) detection kits (Pierce Biotechnology, Rockford, IL, USA) to visualize proteins. Expression of human $\beta$-actin was detected as a loading control.

*2.6. Flow Cytometry Analysis*

*2.6.1. Flow Cytometry Analysis of Apoptosis.* After exposure to the 2 Gy of radiation, HCT116 cells were harvested and double-stained with fluorescein isothiocyanate- (FITC-)

labeled Annexin V and propidium iodide (PI) for 15 minutes in binding buffer according to the manufacturer's instructions to detect cell apoptosis. Then, fluorescence was detected by flow cytometry (Beckman Coulter, Miami, FL, USA) to assay the percentage of cell apoptosis.

*2.6.2. Flow Cytometry Analysis of Intracellular ROS and Mitochondrial ROS.* The ROS assay kit was used to assess intracellular ROS levels. After exposure to 2 Gy of radiation adherent HCT116 cells were washed with serum-free RPMI 1640 medium and stained with 5 $\mu$M of DCFH-DA at 37°C for 30 minutes. Then, labeled HCT116 cells were trypsinized and analyzed by flow cytometry.

MitoSOX™ Red mitochondrial superoxide indicator selectively targets mitochondria to detect mitochondrial ROS. Postirradiation adherent HCT116 cells were washed with serum-free RPMI 1640 medium and incubated with 10 $\mu$M of MitoSOX Red mitochondrial superoxide indicator at 37°C for 30 minutes. After the treatment, HCT116 cells were trypsinized and analyzed by flow cytometry.

*2.6.3. Flow Cytometry Analysis of Mitochondrial Membrane Potential.* One hundred thousand HCT116 cells were collected and washed once with PBS after irradiation. Mitochondrial membrane potential was detected by flow cytometry using a mitochondrial membrane potential assay kit with JC-1. Under normal conditions, JC-1 accumulates in the mitochondrial matrix in the form of J-aggregates, which emit a red fluorescence; however, when the mitochondrial membrane potential collapses, JC-1 exists as a monomer that cannot enter mitochondria and emits a green fluorescence. The ratio of the JC-1 red signal (J-aggregates) to the JC-1 green signal (monomer) was used as a measure of the mitochondrial membrane potential. Data were analyzed by FCS Express V3 software (De Novo Software, Glendale, CA, USA).

*2.7. Immunofluorescence Analysis.* Cells were cultured on coverslips in 35 mm dishes. After the indicated dose of $^{125}$I seeds irradiation, the cells were fixed with 4% formaldehyde in PBS for 15 minutes at 37°C. The fixed cells were permeabilized with 0.2% Triton X-100 in PBS for 15 minutes on ice and subsequently blocked by goat serum. After incubation with primary antibodies overnight at 4°C, LC3 and TIM23 were detected with the polyclonal anti-LC3 antibody and the monoclonal antibody against TIM23, respectively. LC3 were detected with FITC- (Fluorescein Isothiocyanate-) conjugated goat anti-rabbit IgG. TIM23 were labeled with TRITC- (Tetramethylrhodamine Isothiocyanate-) conjugated goat anti-mouse IgG. Nuclei were stained with 4′,6-diamidino-2-phenylindole (Beyotime, China). Fluorescence images were captured with an LSM 510 Zeiss confocal microscope (Carl Zeiss Jena, Germany).

*2.8. Detection of Cellular ATP Levels.* Firefly luciferase-based ATP assay kit (Beyotime, China) was used to measure cellular ATP level. After exposure to the 2 Gy of radiation, HCT116 cells were lysed and centrifuged at 12,000$g$ for 5 minutes. Cell lysates (100 $\mu$L) were mixed with 100 $\mu$L of ATP detection working dilution in a 96-well plate, and the cellular ATP levels were measured using the BioTek Synergy 2 Microplate Reader (BioTek Instruments Inc., Winooski, VT, USA). A BCA assay kit was used to determine the protein concentration of cell lysates (1 $\mu$L) of each group. The ratio of cellular ATP level to the protein concentration was used to evaluate total ATP level.

*2.9. Reverse Transcription and Real-Time PCR.* Total RNA was extracted from cells using Trizol (Invitrogen, Carlsbad, CA, USA) according to the manufacturer's instructions, and 1 $\mu$g of total RNA was used to reverse transcribe cDNA. Real-time PCR was performed using multiple kits (SYBR Premix Ex TaqTM, DRR041A, Takara Bio) on CFX96 (Bio-Rad, Hercules, CA, USA) [29]. The housekeeping gene hypoxanthine phosphoribosyl transferase (HPRT) was used as an endogenous control. The following primers were used: HPRT upstream primer 5′-CAGTATAATCCAAAGATGGTCAA-3′ and HPRT downstream primer 5′-TTAGGCTTTGTATTTTGCTTTTCC-3′; BNIP3 upstream primer 5′-CAGGGCTCCTGGGTAGAACT-3′ and BNIP3 downstream primer 5′-CTACTCCGTCCAGACTCATGC-3′; NIX upstream primer 5′-ATGTCGTCCCACCTAGTCGAG-3′ and NIX downstream primer 5′-TGAGGATGGTACGTGTTCCAG-3′; HIF-1$\alpha$ upstream primer 5′-GAACGTCGAAAAGAAAAGTCTCG-3′, and HIF-1$\alpha$ downstream primer 5′-CCTTATCAAGATGCGAACTCACA-3′.

*2.10. Cell Transfection.* LC3-specific siRNAs (small interference RNA) (5′-GAGUGAGCUCAUCAAGAUAtt-3′) and an unrelated control siRNA (5′-UUCUCCGAACGUGUCACGUtt-3′) [30] were synthesized from GenePharma Co., Ltd., to knockdown of LC3 expression. HCT116 cells were transfected with 100 nM LC3 siRNA or nonrelated control siRNA. Transfections were performed with LipofectamineTM 2000 in accordance with the manufacturer's instruction.

*2.11. Statistical Analysis.* Experiments were performed at least three times in duplicate. Statistical analyses were performed using the statistical software SPSS 17.0 (SPSS Inc., Chicago, IL, USA). The two-tailed $t$-test was applied to compare group means. Statistical significance was set at $p \leq 0.05$.

## 3. Results

*3.1. Inhibition of Autophagy Enhanced the Sensitivity of Tumor Cells to $^{125}$I Seeds Radiation.* To investigate how autophagy affects the radiosensitivity of tumor cells, clonogenic survival assay was performed to assess the response to $^{125}$I seeds radiation with and without pretreatment with autophagy inhibitors. HCT116 cells were pretreated with the autophagy inhibitors 3-MA (0.5 mM) or Ly294002 (10 $\mu$M) 2 hours prior to being exposed to 2 Gy and 4 Gy $^{125}$I seeds radiation. The ratios of surviving fraction between 3MA group and control group were 0.81, 0.48 for total doses of 2 and 4 Gy, respectively (Figure 1(a)). What is more, the ratios of surviving fraction between Ly294002 and control group were 0.83 and 0.59 for total doses of 2 and 4 Gy, respectively (Figure 1(b)). We found a statistically significant decrease in the clonogenic survival

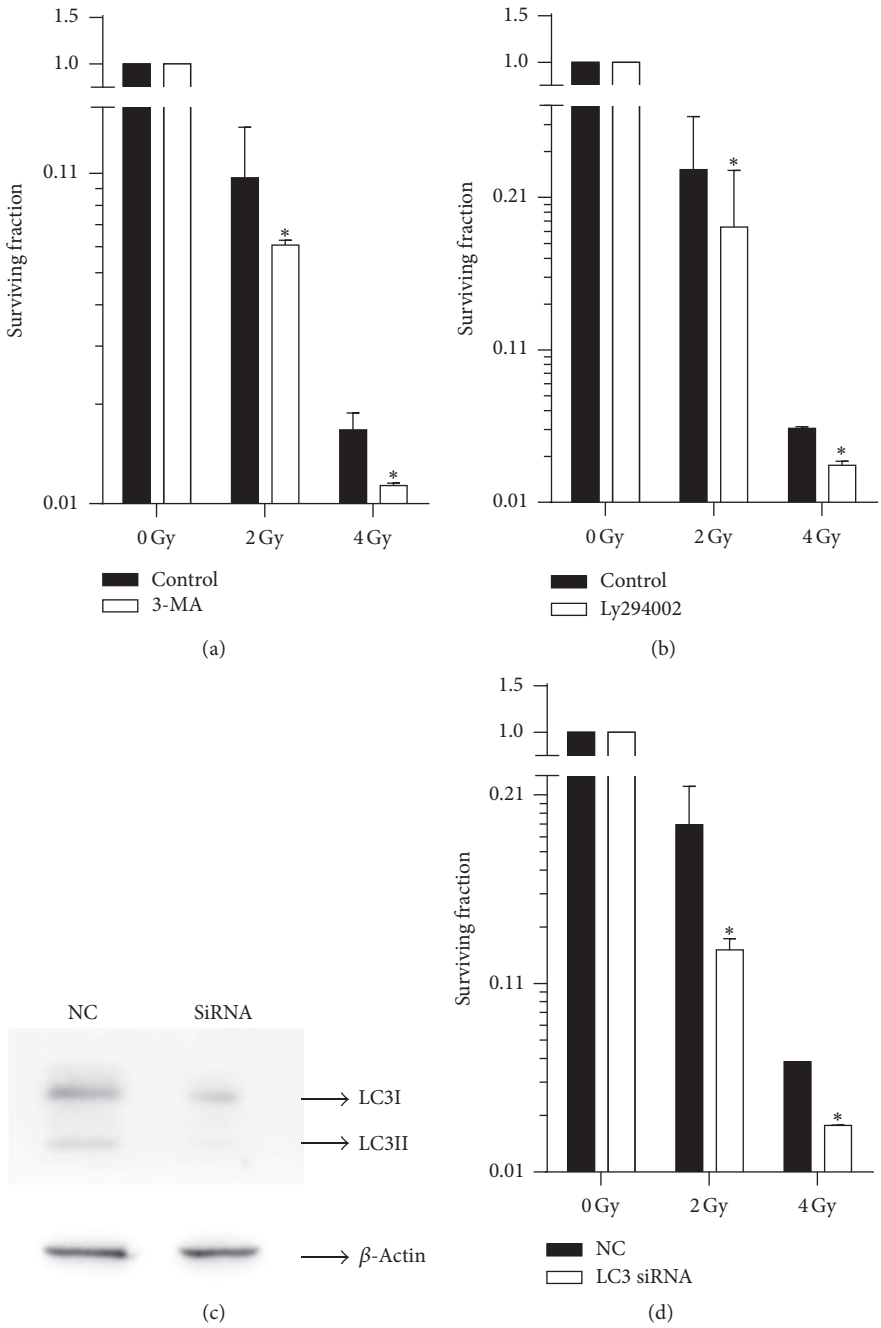


Figure 1: Inhibition of autophagy enhanced the sensitivity of HCT116 cells to $^{125}$I seeds radiation. (a) HCT116 cells were pretreated with or without 3-MA before exposure to the indicated dose of $^{125}$I seeds radiation. Clonogenic survival was assessed in the presence or and absence of 3-MA. (b) Clonogenic survival was assessed in HCT116 cells pretreated with or without Ly294002 before exposure to the indicated dose of $^{125}$I seeds radiation. (c) HCT116 cells were transfected with LC3 siRNA or unrelated control siRNA. Western blot was performed to assess the expression of LC3 48 h after transfection. Representative Western blot analysis of LC3II/I is shown. (d) Clonogenic survival was assessed in HCT116 cells transfected with LC3 siRNA or unrelated control siRNA before exposure to the indicated dose of $^{125}$I seeds radiation. The values are the means ± SD of three independent experiments. The two-tailed $t$-test was used for comparing the means. $*$ indicates significant difference ($p \leq 0.05$) as compared to the control group.

fraction in HCT116 cells pretreated with 3-MA or Ly294002 at 2 Gy and 4 Gy ($p \leq 0.05$), suggesting that these autophagy inhibitors have a radiosensitizing effect on HCT116 cells. Neither 3-MA nor Ly294002 was specific autophagy inhibitor. We further investigated whether knockdown of LC3 expression, a conserved gene required for mammalian autophagy, affected the radiosensitivity of HCT116 cells. Clonogenic survival assay was used to assess the response to $^{125}$I seeds

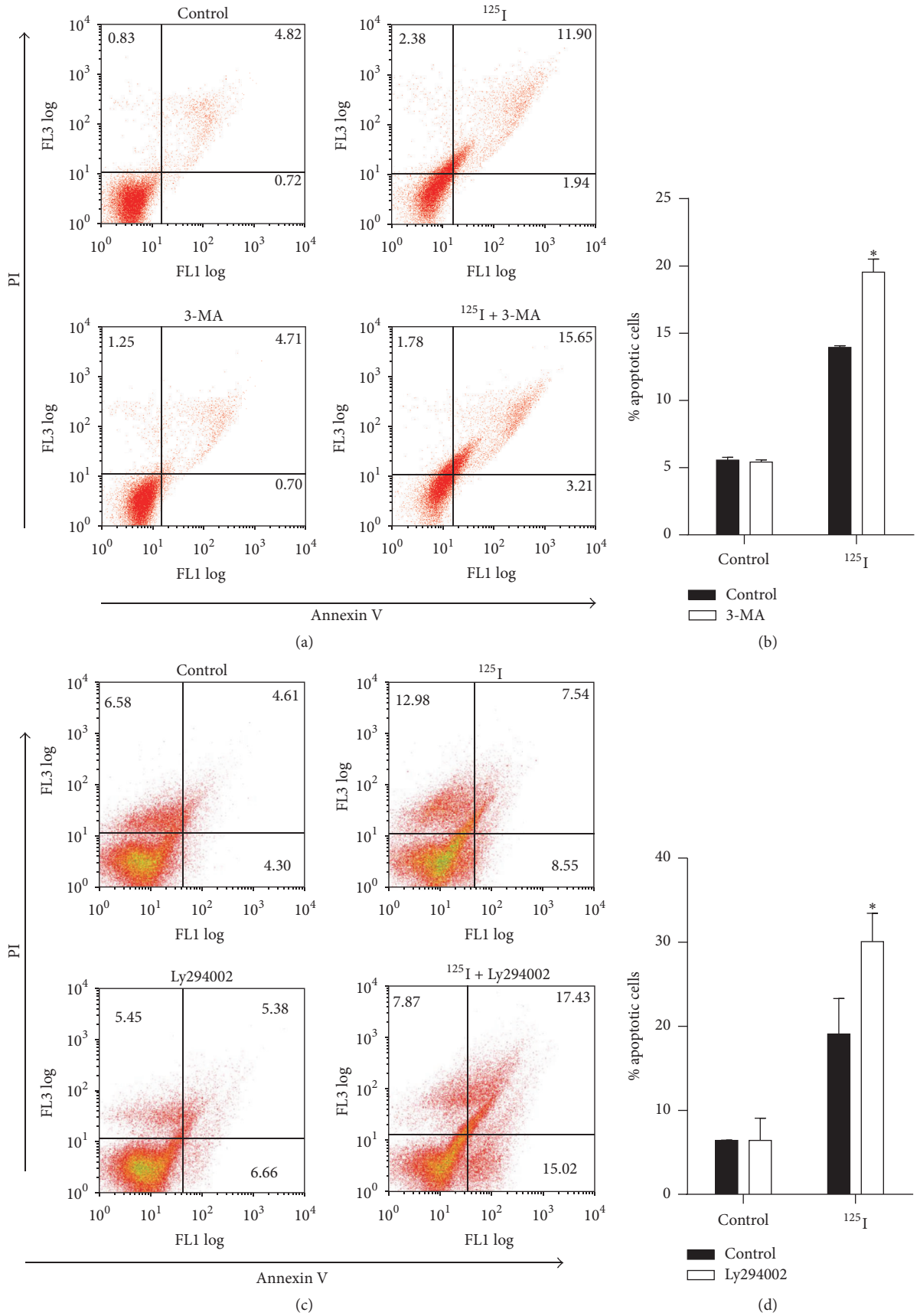


Figure 2: Continued.

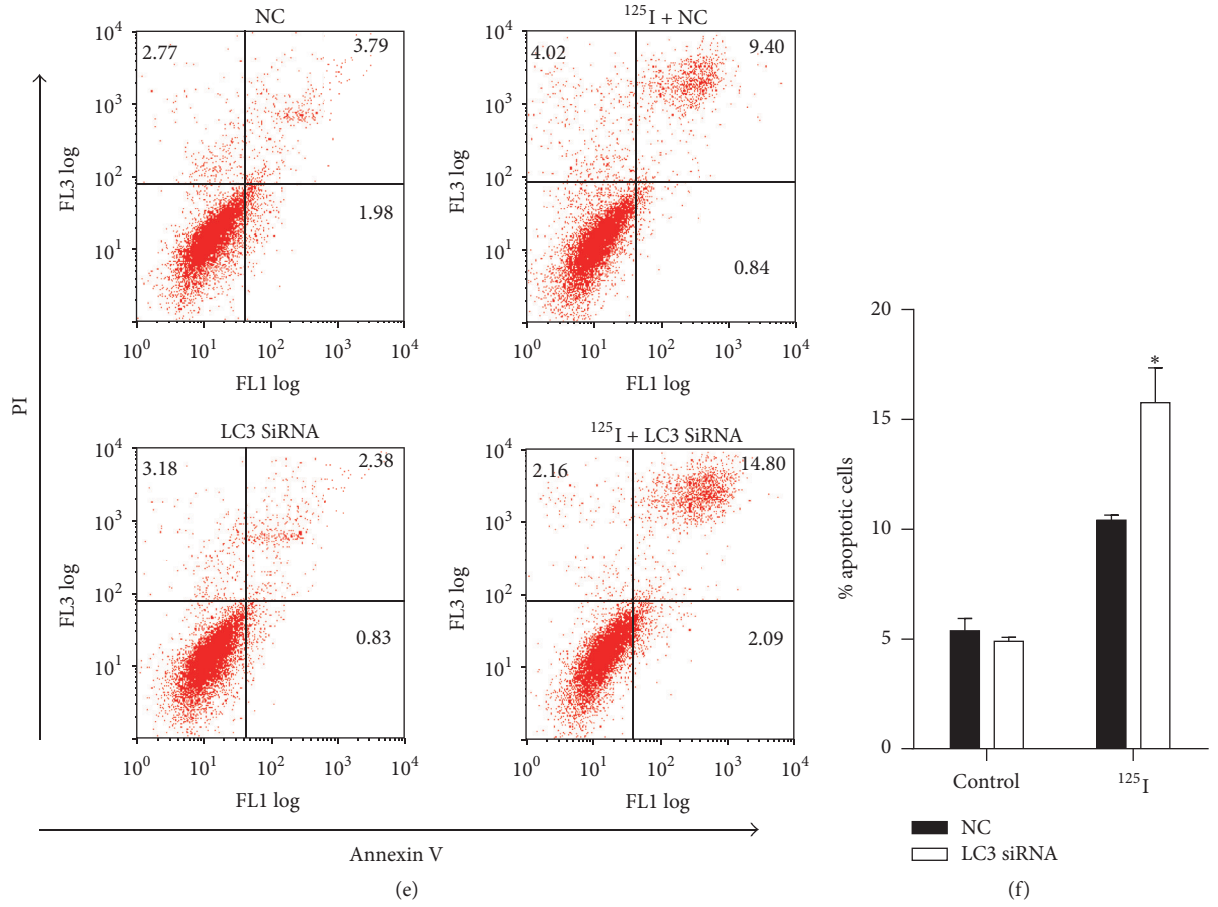


Figure 2: Inhibition of autophagy promoted apoptosis induced by $^{125}$I seeds radiation. (a) Representative example of flow cytometry analysis pretreated with and without 3-MA before exposure to indicated doses of $^{125}$I seeds radiation. Apoptotic cell death was detected by Annexin V and PI double staining. (b) The percentage of apoptosis with and without 3-MA was examined by flow cytometry after Annexin V and PI double staining. Annexin $V^+/PI^-$ cell and anexin $V^+/PI^+$ cell populations were quantified and analyzed. (c) Typical example of flow cytometry analysis pretreated with and without Ly294002 before exposure to indicated doses of $^{125}$I seeds radiation. (d) The percentage of apoptosis with and without Ly294002 was measured by flow cytometry with Annexin V and PI double staining. Annexin $V^+/PI^-$ cell and anexin $V^+/PI^+$ cell populations were quantified and analyzed. (e) Typical example of flow cytometry analysis in HCT116 cells transfected with LC3 siRNA or unrelated control siRNA before exposure to the indicated dose of $^{125}$I seeds radiation. (f) The percentage of apoptosis in HCT116 cells transfected with LC3 siRNA or unrelated control siRNA was measured by flow cytometry with Annexin V and PI double staining. Annexin $V^+/PI^-$ cell and anexin $V^+/PI^+$ cell populations were quantified and analyzed. $*$ indicates significant difference ($p \leq 0.05$) between treated group or untreated group.

radiation after transfection with LC3 siRNA or nonrelated control siRNA duplex. The expression of LC3 in HCT116 cells transfected with LC3 siRNA duplex significantly decreased compared to nonrelated control siRNA group (Figure 1(c)). Following irradiation the ratios of surviving fraction between LC3 siRNA group and nonrelated control siRNA were 0.66, 0.51 for total doses of 2 and 4 Gy, respectively. We found that knockdown of LC3 expression sensitized HCT116 cells to $^{125}$I seeds radiation at 2 Gy and 4 Gy ($p \leq 0.05$, Figure 1(d)), suggesting that inhibition of autophagy had a radiosensitizing effect on HCT116 cells.

*3.2. Inhibition of Autophagy Promoted Apoptosis Induced by $^{125}$I Seeds Radiation.* In previous studies we had shown that $^{125}$I seeds radiation induces apoptosis in colorectal cancer cells. To examine whether the enhanced radiosensitivity of autophagy inhibitors was due to increased apoptosis, the percentage of apoptotic cells was measured by double staining with Annexin V and PI and assayed by flow cytometry. We found that the proportion of $PI^-$/Annexin $V^+$ and $PI^+$/Annexin $V^+$ cell population in HCT116 cells increased from 13.9% to 19.5% following treatment with $^{125}$I seeds radiation plus the autophagy inhibitor 3-MA ($p \leq 0.05$, Figures 2(a) and 2(b)). To confirm this phenomenon, the same experiments were duplicated with autophagy inhibitor Ly294002 instead of 3MA (Figure 2(c)). The percentage of apoptosis increased from 19.1% to 30.1% in cells treated with $^{125}$I seeds radiation plus Ly294002 ($p \leq 0.05$, Figure 2(d)). We further investigated whether LC3 siRNA affected the apoptosis of HCT116 cells induced by $^{125}$I seeds radiation. After transfection with LC3 siRNA duplex, the percentage of apoptotic cell induced by $^{125}$I seeds radiation increased from 10.41 to 15.77

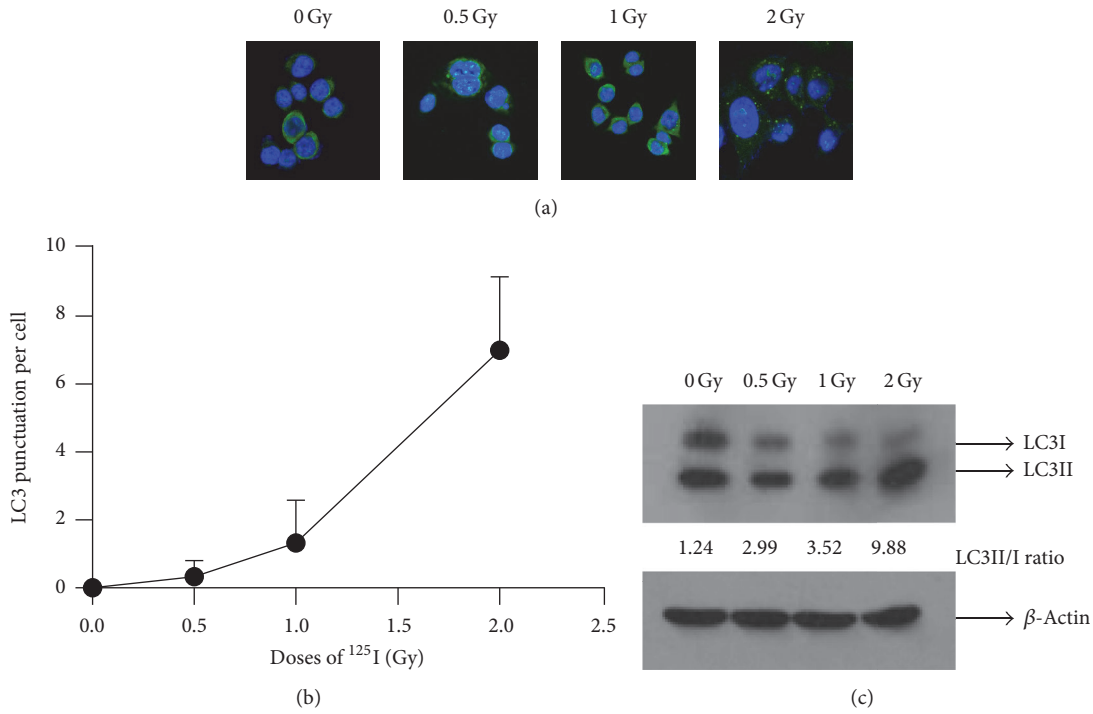


Figure 3: $^{125}$I seeds radiation induced autophagy in HCT116 cells. (a) HCT116 cells were exposed to the indicated dose of $^{125}$I seeds radiation. LC3 punctuation was measured using immunofluorescence with polyclonal anti-LC3 antibody. DAPI was used to stain nuclei. (b) The number of LC3 punctuations per cell after exposure to indicated doses of $^{125}$I seeds radiation was quantified. The values are the mean (±SD) of at least three different cells. (c) HCT116 cells were exposed to the gradually increased dose of $^{125}$I seeds radiation. The ratio of LC3II/I was analyzed by Western analysis with anti-LC3 antibody. $\beta$-Actin was evaluated as a loading control.

($p \leq 0.05$, Figures 2(e) and 2(f)). These results suggested that inhibition of autophagy increased the sensitivity to $^{125}$I seeds radiation by enhancing apoptosis.

*3.3. $^{125}$I Seeds Radiation Induced Mitophagy in Tumor Cells.* To investigate whether $^{125}$I seeds radiation could induce autophagy in HCT116 cells, LC3-I and LC3-II were used as autophagy markers to estimate the induction of autophagy and the overall autophagic flux to permit correct interpretation of the results. Immunofluorescence staining with anti-LC3 antibody was performed with HCT116 cells following exposure to 0, 0.5, 1, and 2 Gy of $^{125}$I seeds radiation (Figure 3(a)). As shown in Figure 3(b), the number of LC3 punctuations per cell increased gradually after exposure to 0, 0.5, 1, and 2 Gy of $^{125}$I seeds radiation. Western blot analysis, performed to examine the transformation of soluble LC3 (LC3-I) to the LC3-II form, showed that the ratio of LC3-II to LC3-I increased gradually after treatment with indicated doses of $^{125}$I seeds radiation (Figure 3(c)). This provided further evidence that $^{125}$I seeds radiation induced autophagy in a dose-dependent manner in HCT116 cells.

Autophagy involves two key processes: the formation of autophagosomes and the formation of autolysosomes. In the initial stage, membrane distant from either the Golgi or ER sequesters cellular components to form autophagosome. At a relatively late stage of autophagy, autophagosome fuses with the lysosome to form an autolysosome, where LC3-II and sequestered cellular components were degraded by lysosomal hydrolytic enzymes [31–33]. There are two causes for the accumulation of LC3-II: one is increase of autophagosome formation and the other is inhibition of the formation of autolysosomes which is the site for degradation of autophagosomes [34]. To identify which of these two mechanisms was responsible for the autophagy caused by $^{125}$I seeds radiation, we then investigated whether elevated LC3-II levels were due to the upregulation of autophagosome formation or the escape of autophagosome-lysosome fusion. Chloroquine (CQ), which acts as a late-stage autophagy inhibitor by blocking autophagosome-lysosome fusion, was used to treat the irradiated HCT116 cells for 6 hours before harvest, and the cells were examined under a confocal microscope (Figure 4(a)). As expected, treatment with CQ could make further increase of the number of LC3-II punctuations per cell induced by $^{125}$I seeds radiation ($p \leq 0.05$, Figure 4(b)). Moreover, whole cell lysates from treated cells were analyzed by Western blotting in parallel at the same time. The results showed that CQ could make further increase of the ratio of LC3-II to LC3-I induced by $^{125}$I seeds radiation (Figure 4(c)). These suggested that $^{125}$I seeds radiation induced LC3-II punctuation accumulation was due to the increase of autophagosome formation rather than inhibition of lysosome-autophagosome fusion.

We also used electron microscopy, the gold standard for detecting autophagy, to investigate whether $^{125}$I seeds radiation induced autophagy in HCT116 cells. Transmission electron microscope (TEM) analysis revealed that a large number

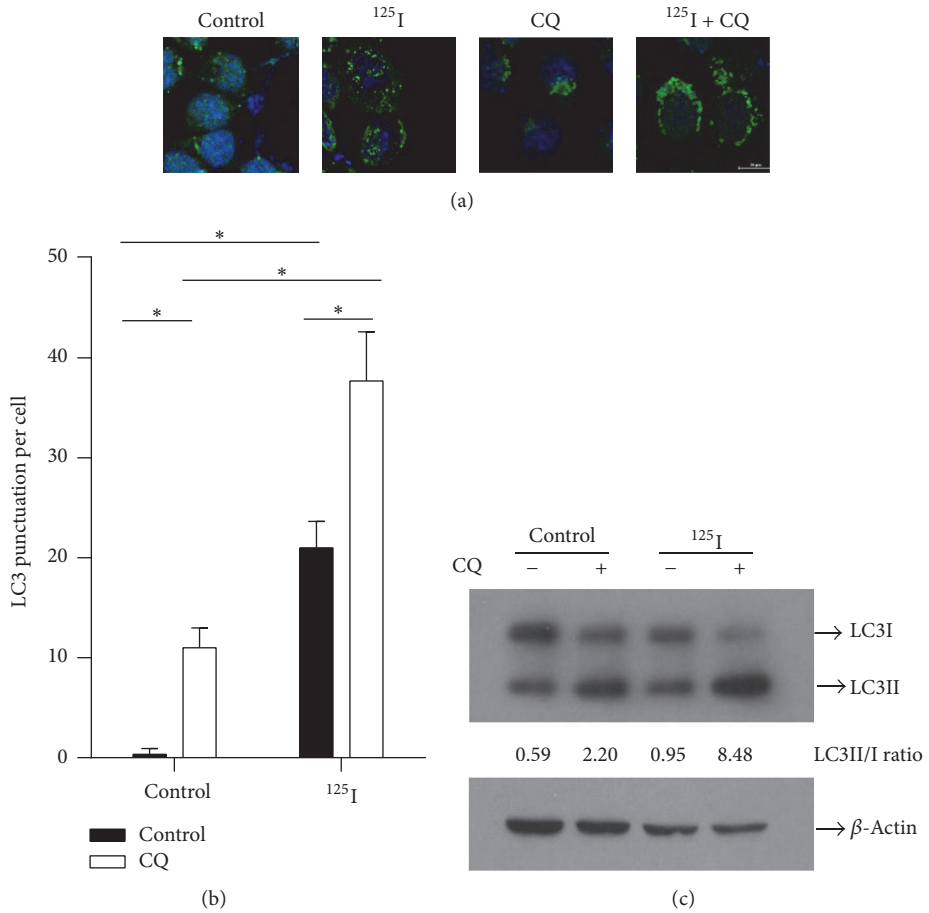


Figure 4: $^{125}$I seeds radiation promoted autophagosome formation in HCT116 cells. (a) Irradiated HCT116 cells were treated with or without 40 $\mu$mol of chloroquine for 6 hours. LC3 punctuations were detected using immunofluorescence and images were captured by a confocal microscope. (b) The percentage of LC3 punctuation per cell was quantified. The values are the means ± SD of at least three different cells. (c) HCT116 cells were exposed to 125I seeds radiation (2 Gy) with or without chloroquine for 6 hours, respectively. The ratio of LC3II/I was measured by Western blotting analysis. $*$ indicates significant difference ($p \leq 0.05$) as compared to the control group.

of mitochondria in autophagosome-like vacuoles appeared in the cytoplasm after exposure to 2 Gy of $^{125}$I seeds radiation (Figure 5(a)). This phenomenon was consistent with the result of immunofluorescence analysis. Following exposure to 2 Gy of $^{125}$I seeds radiation, the cells were double indirect immunofluorescence staining with an anti-TIM23 antibody (red) and an anti-LC3 antibody (green) to detect the mitochondrial marker protein TIM23 and autophagosome marker protein LC3, respectively. The confocal image showed LC3 punctuation colocalized with mitochondria after $^{125}$I seeds radiation. Besides, this colocalization induced by $^{125}$I seeds radiation increased significantly after treatment with CQ, which could block autophagosome-lysosome fusion to amplify autophagy (Figure 5(b)). These results further supported that $^{125}$I seeds radiation induced robust mitophagy by promoting autophagosome formation.

*3.4. $^{125}$I Seeds Radiation Impaired Mitochondria and Induced Oxidative Stress.* To study whether $^{125}$I seeds radiation could induce mitochondrial damage, we examined a series of indices that can reflect mitochondrial dysfunction. Immunofluorescence staining was performed with anti-TIM23 antibody to detect the mitochondrial marker protein TIM23. The fluorescence confocal image showed that $^{125}$I seeds radiation induced changes in mitochondrial morphology, altering it from the elongated linear network form to a floccular and dot form (Figure 6(a)). In addition, mitochondrial membrane potential was analyzed with flow cytometry (Figure 6(b)); we found that $^{125}$I seeds radiation impaired mitochondrial function and induced decrease in mitochondrial membrane potential ($p \leq 0.05$, Figure 6(c)).

It has been reported that mitochondrial dysfunction induced by radiation results in reduction of ATP synthesis owing to disruption of the proton gradient across the mitochondrial membrane [35, 36]. We next investigated whether $^{125}$I seeds radiation induced mitochondrial dysfunction led to alterations in ATP production. Cellular ATP level was evaluated by firefly luciferase-based ATP assay kit; the results showed the level of total ATP decreased significantly after

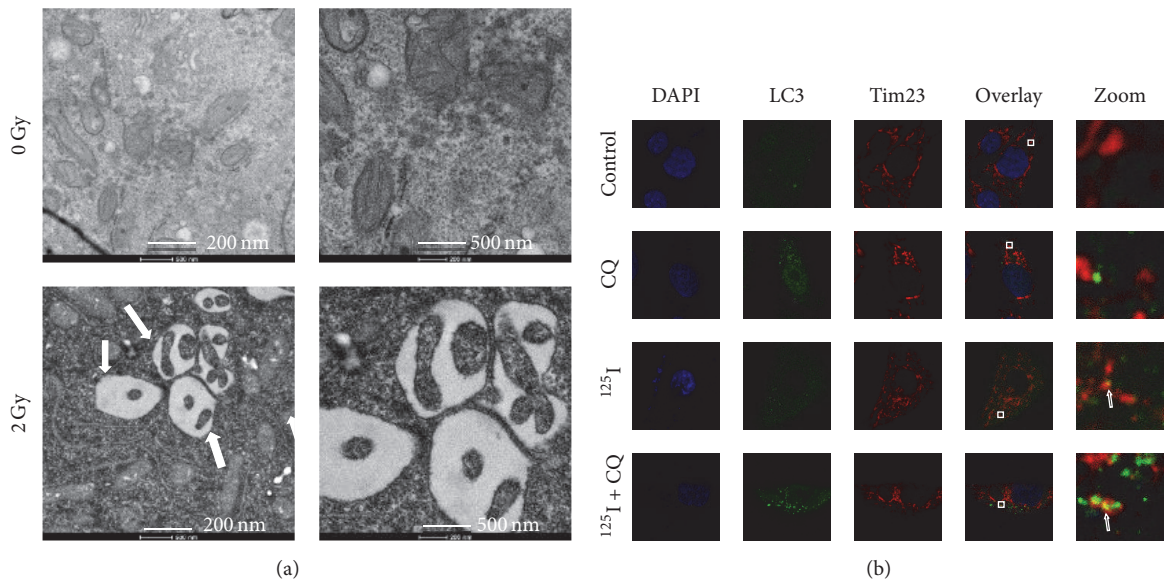


FIGURE 5: $^{125}$I seeds radiation induced mitophagy in HCT116 cells. (a) HCT116 cells were exposed to $^{125}$I seeds radiation (2 Gy); the representative transmission electron microscopic ultrastructures are shown. The arrows indicate an autophagic vacuole containing mitochondria (scale bars 200 nm and 500 nm). (b) HCT116 cells were exposed to $^{125}$I seeds radiation alone or in combination with CQ (40 $\mu$mol) for 6 hours. Following fixation, the cells were immunostained with an anti-TIM23 antibody (red) and an anti-LC3 antibody (green) and visualized by confocal microscopy. The representative confocal microscopy images are shown. Small squares denoted the area zoomed in region of the images and white arrows denoted mitophagy punctuation induced by $^{125}$I seeds radiation.

$^{125}$I seeds radiation ($p \leq 0.05$, Figure 6(d)). After exposure to 2 Gy of $^{125}$I seeds radiation, cells were stained with the mitochondrial ROS and subjected to flow cytometry analysis (Figure 6(e)). Results showed that $^{125}$I seeds radiation elevated levels of mitochondrial ROS in HCT116 cells ($p \leq 0.05$, Figure 6(f)). Similarly, postirradiation cells were stained with the intracellular ROS probes and analyzed by flow cytometry (Figure 6(g)). Results showed that $^{125}$I seeds radiation elevated levels of intracellular ROS in HCT116 cells ($p \leq 0.05$, Figure 6(h)). Together, these data suggested that $^{125}$I seeds radiation induced oxidative damage in mitochondria.

*3.5. Elevated ROS Is Critical for Both Mitophagy and Apoptosis Induced by $^{125}$I Seeds Radiation.* There is increasing evidence that oxidative stress is responsible for autophagy [25]. To confirm the role of ROS in mitophagy and apoptosis induced by $^{125}$I seeds radiation, we treated HCT116 cells with N-acetyl-L-cysteine (NAC; a ROS scavenger), $^{125}$I seeds radiation, or both. Mitochondrial ROS and intracellular ROS generation were then analyzed using the corresponding probe for flow cytometry analysis. As shown in Figure 7(a), NAC decreased $^{125}$I seeds radiation induced accumulation of mitochondrial ROS. Statistical results from three independent experiments in duplicate are shown in Figure 7(b) ($p \leq 0.05$). Besides, NAC decreased accumulation of intracellular ROS induced by $^{125}$I seeds radiation (Figure 7(c)). Experiments were duplicated three times and data are shown in Figure 7(d) ($p \leq 0.05$). Protein levels of LC3-II and LC3-1 were determined by Western blotting in parallel. As shown in Figure 7(e), the rise in ratio of LC3-II to LC3-1 that was induced by $^{125}$I seeds radiation lowered when the cells were treated with NAC. Moreover, immunofluorescence staining showed that NAC could decrease the LC3 punctuation accumulation induced by $^{125}$I seeds radiation (Figure 7(h)).

We next utilized mitochondrial respiratory chain inhibitor to investigate the role of mitochondrial ROS on mitophagy induced by $^{125}$I seeds radiation. DPI (50 uM) and Antimycin A (50 uM), which act as mitochondrial respiratory chain inhibitor by blocking electron flow at mitochondrial respiratory chain complexes I and III, respectively, were used to treat the irradiated HCT116 cells for 18 hours before harvest. As shown in Figures 6(f)–6(h), the treatment of DPI and Antimycin A could promote the accumulation of mitochondrial ROS and further increase mitophagy induced by $^{125}$I seeds radiation.

We also used NAC, the ROS scavenger, to examine whether apoptosis correlated with the level of ROS induced by $^{125}$I seeds radiation. Cells were doubled stained with the probes Annexin V and PI to evaluate the percentage of apoptosis by flow cytometry analysis (Figure 8(a)). Flow cytometry analysis showed that NAC decreased the proportion of apoptosis induced by $^{125}$I seeds radiation ($p \leq 0.05$, Figure 8(b)), indicating that ROS play an important role in mitophagy and apoptosis in HCT116 cells.

*3.6. The Accumulation of Mitochondrial ROS Induced by $^{125}$I Seeds Irradiation Is Critical for mRNA Expression of HIF-1$\alpha$ and BNIP3/NIX.* We investigated whether $^{125}$I seeds radiation influenced the expression of HIF-1$\alpha$ and its target genes. Real-time PCR was performed to detect the expression of HIF-1$\alpha$ and its target genes BNIP3 and NIX. As shown in

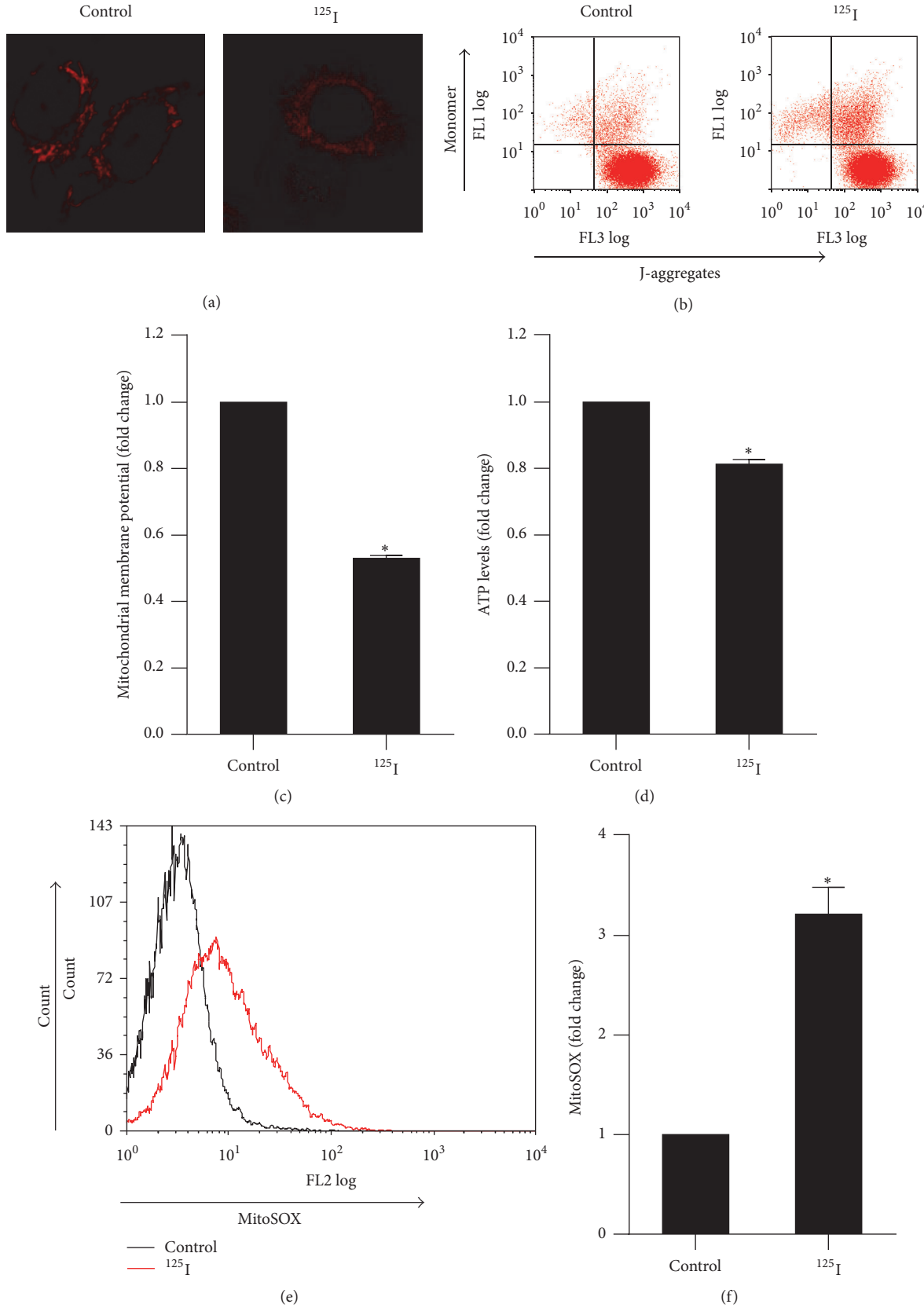


Figure 6: Continued.

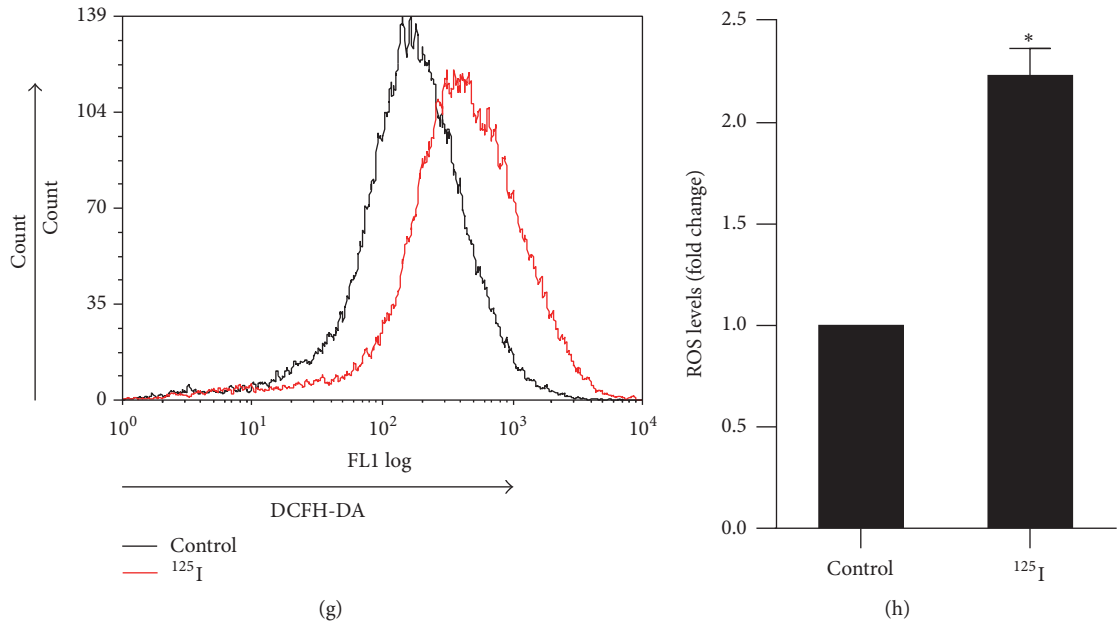


Figure 6: $^{125}$I seeds radiation induced oxidative damage in mitochondria. HCT116 cells were exposed to 2 Gy of $^{125}$I seeds radiation. (a) The cells were fixed and stained with anti-Tim23 antibody, and images were captured by a confocal microscope. The representative images are shown (scale bar 10 $\mu$m). (b) The mitochondrial potential was analyzed by flow cytometry with a JC-1 probe. Typical example of flow cytometry analysis was shown. (c) The ratio of J-aggregates and JC-1 monomers was used to evaluate the mitochondrial potential. The values are the means ± SD of three independent experiments. (d) Total ATP was evaluated by an ATP assay kit. The values are the means ± SD of three independent experiments. (e) Mitochondrial ROS were analyzed by flow cytometry after staining with MitoSOX. Typical example of flow cytometry analysis was shown. (f) Quantitative analysis of mitochondrial ROS. The values were derived from mean fluorescence intensity. The values are the means ± SD of three independent experiments. (g) Intracellular ROS were stained by DCFH-DA and analyzed by flow cytometry. (h) Quantitative analysis of intracellular ROS. The values were derived from mean fluorescence intensity. The values are the means ± SD of three independent experiments. $^*p \le 0.05$, as compared to the control group.

Figures 9(a)–9(c), $^{125}$I seeds radiation significantly upregulated the mRNA expression of HIF-1$\alpha$ ($p \le 0.05$, Figure 9(a)), BNIP3 ($p \le 0.05$, Figure 9(b)), and NIX ($p \le 0.05$, Figure 9(c)).

To determine whether ROS induced by $^{125}$I seeds radiation can raise the expression of BNIP3 and NIX, which is a crucial signal transduction pathway to regulate mitophagy, we examined the expression of HIF-1$\alpha$, BNIP3, and NIX at the mRNA level by using real-time PCR. As shown in Figure 9, NAC decreased the expression of HIF-1$\alpha$ ($p \le 0.05$, Figure 9(d)), BNIP3 ($p \le 0.05$, Figure 9(e)), and NIX ($p \le 0.05$, Figure 9(f)). And the treatment of Antimycin A could further increase the mRNA expression of HIF-1$\alpha$ ($p \le 0.05$, Figure 9(g)), BNIP3 ($p \le 0.05$, Figure 9(h)), and NIX ($p \le 0.05$, Figure 9(i)) induced by $^{125}$I seeds radiation, indicating that mitochondrial ROS induced by $^{125}$I seeds irradiation might be critical for mitophagy and apoptosis through HIF-1$\alpha$–BNP3/NIX pathways.

## 4. Discussion

Presently available evidence is in favor of autophagy as a novel cancer therapy target [37]. Autophagy is a dynamic process characterized by lysosomal degradation of cytoplasmic components such as cytoplasmic proteins and intracellular organelles [38]. The process requires the formation of the double-membrane autophagosome, which sequesters and transports the cytoplasmic cargo to the lysosome for degradation [39]. Recent studies show that autophagy plays an important role in cancer cell fate decisions following stress condition such as starvation, hypoxia, and chemotherapy [40]. Several studies have shown that elevated level of autophagy is associated with radio-resistance of various cancers [41, 42]. Multiple clinical trials have been performed to study the effects of conventional anticancer radiotherapy combined with autophagy inhibitors [37]. A number of autophagy inhibitors, such as chloroquine (CQ), hydroxychloroquine (HCQ), and 3-methyladenine (3-MA), have been applied in clinical trials. The combination of autophagy inhibitors and radiotherapy has been shown to provide survival benefits and increased lifespan in patients with cancer [43–45]; however, the specific role of autophagy induced by $^{125}$I seeds radiation has not yet been determined.

In the present study, we first showed that both autophagy inhibitors 3-MA and Ly294002 could decrease the survival fraction of HCT116 cells after $^{125}$I seeds radiation (Figures 1(a) and 1(b)). Moreover, knockdown of LC3 expression sensitizes HCT116 cells to $^{125}$I seeds radiation, indication that inhibition of autophagy has a radiosensitizing effect on HCT116 cells (Figure 1(d)). Next, we explored how autophagy inhibitors

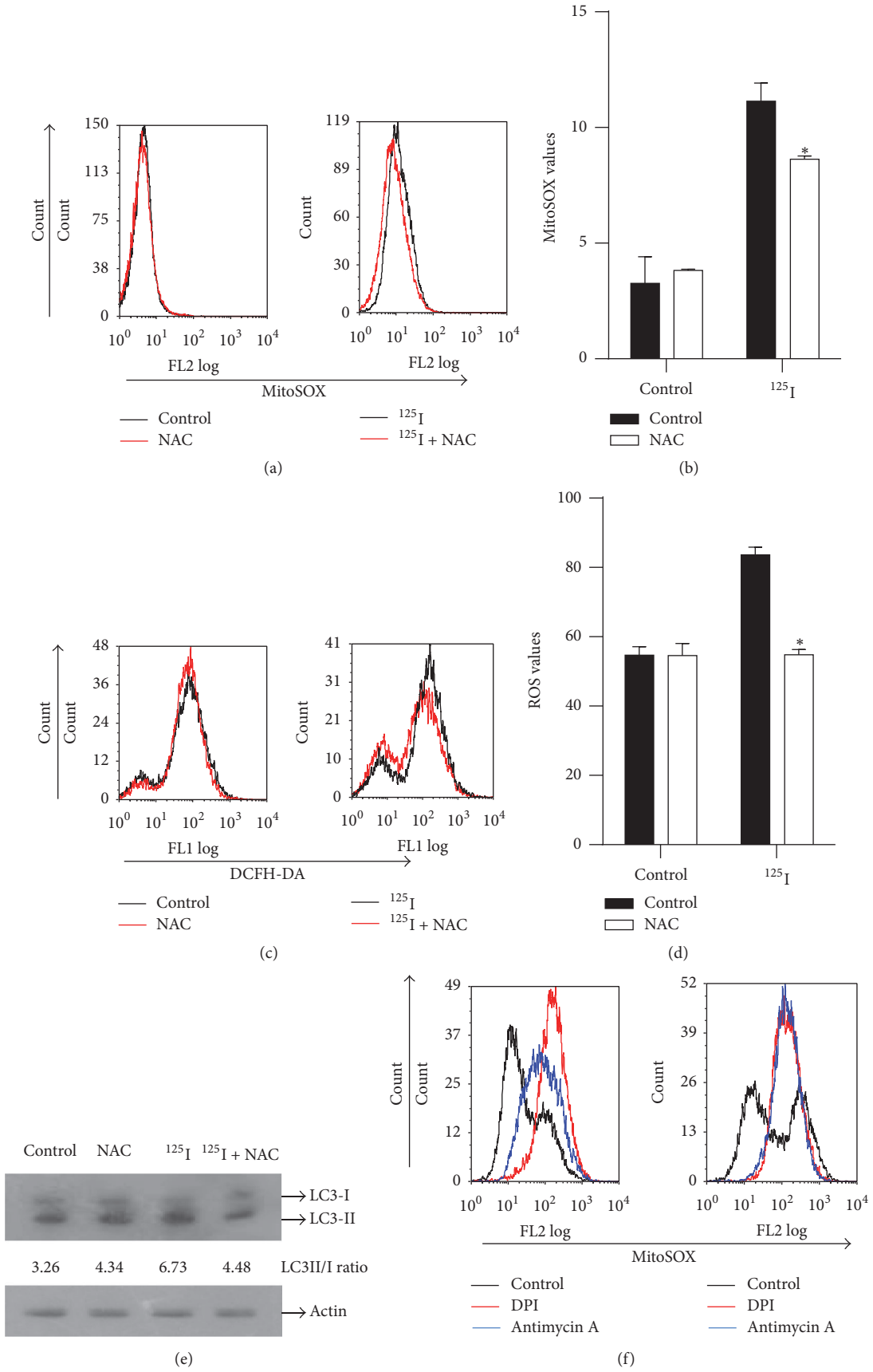


Figure 7: Continued.

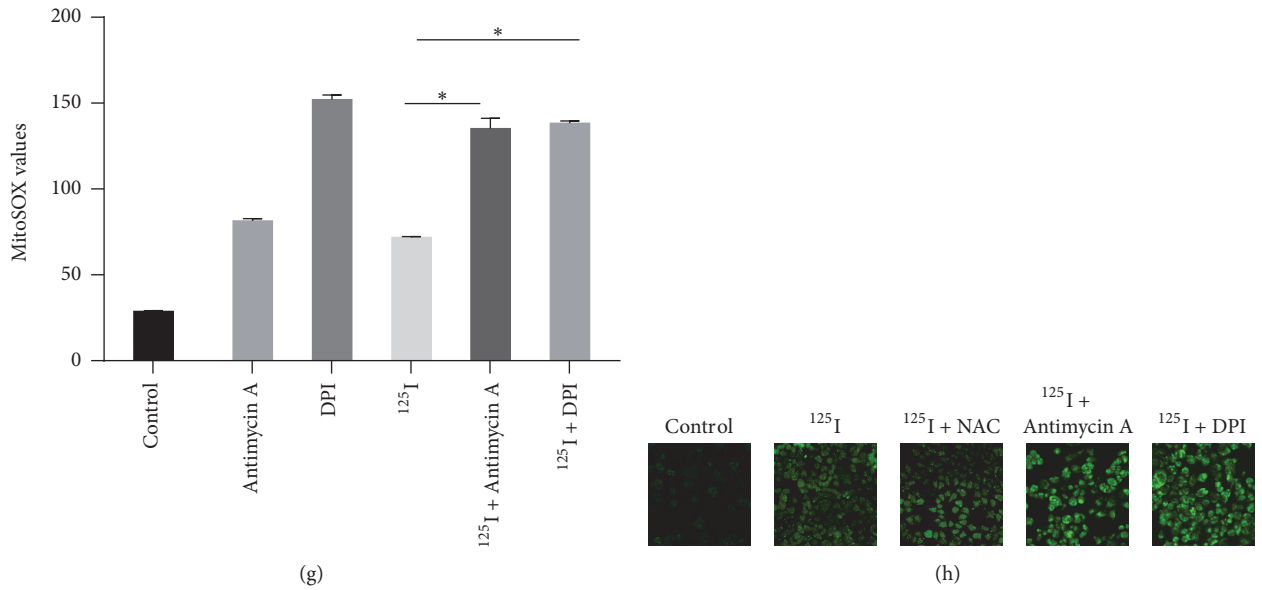


Figure 7: Accumulation of mitochondrial ROS is critical for $^{125}$I seeds radiation induced mitophagy. (a–e) HCT116 cells were incubated with and without 5 mM of NAC for 4 hours and then either mock exposed or exposed to 2 Gy of $^{125}$I seeds radiation. (a) Cells were stained with MitoSOX probe and then mitochondrial ROS were measured using flow cytometry. Typical example of flow cytometry analysis was shown. (b) Quantitative analysis of mitochondrial ROS. The values were derived from mean fluorescence intensity. The values are the means ± SD of three independent experiments. (c) Cells were stained by DCFH-DA probe and intracellular ROS were measured using flow cytometry. Typical example of flow cytometry analysis was shown. There are two peaks in the images which represented DCFH-DA negative peak and DCFH-DA positive peak, respectively. (d) Quantitative analysis of intracellular ROS. The values were derived from mean fluorescence intensity. (e) Representative Western blot analysis of LC3II/I is shown. (f–h). HCT116 cells were exposed to $^{125}$I seeds radiation with or without Antimycin A (50 uM) or DPI (50 uM) for 18 hours. (f) Flow cytometry was performed to measure mitochondrial ROS with MitoSOX probe. Typical example of flow cytometry analysis was shown. (g) Quantitative analysis of mitochondrial ROS. The values were derived from mean fluorescence intensity. (h) Cells were immunostained with anti-LC3 antibody (green) and visualized by confocal microscopy. The typical confocal microscopy images are shown. The values are the means ± SD of three independent experiments. ∗ indicates a significant difference ($p \leq 0.05$) as compared to the control group.

modified the response of HCT116 cells to $^{125}$I seeds radiation. We found that inhibition of autophagy increased the proportion of apoptosis induced by $^{125}$I seeds radiation (Figures 2(a)–2(f)). Autophagy induced by multiple forms of cellular stress—such as hypoxia, ROS accumulation, DNA damage, protein aggregates, damaged organelles, or intracellular pathogens—interact with apoptosis to control cell survival and death [46]. We therefore consider it possible that $^{125}$I seeds radiation triggers autophagy to protect colorectal cancer cells from apoptotic cell death.

LC3 is an important marker for detection of autophagy. It exists in two forms: LC3-I and LC3-II. LC3-I, a soluble cytosolic protein, is initially synthesized in an unprocessed form, proLC3. Once autophagy is triggered, LC3-I is modified to LC3-II which is recruited to autophagosomal membranes and showed punctuation-like distribution. The amount of LC3-II punctuation is reliably correlated with the extent of autophagosome formation [47]. LC3 lipidation can be evaluated by observing the ratio of LC3-II to LC3-1 on immunoblots. The accumulation of autophagosome can be measured by TEM image analysis or immunofluorescence analysis of LC3 punctuation [34]. In the present study, we identified $^{125}$I seeds radiation induced autophagy (Figures 3(a)–3(c)) and autophagic flux (Figures 4(a)–4(c)) by immunofluorescence and Western blotting for the lipidation of LC3, respectively. Furthermore, the TEM images revealed the presence of autophagic vacuoles with mitochondria inside (Figure 5(a)), which was consistent with the results of immunofluorescence analysis (Figure 5(b)). On the basis of these findings we concluded that $^{125}$I seeds radiation robustly induced mitophagy.

Mitophagy is a cargo-specific autophagy that selectively removes damaged mitochondria [48]. As a cell death executor, in addition to its more traditional roles in bioenergetics and metabolism, mitochondria are now recognized to play an important role in radiation induced cellular responses [11]. Mitochondrial damage could induce mitophagy to control mitochondrial number and quality to match metabolic demands [49]. Mitochondria are crucial energy organelles where large amounts of ATP are produced using the electrochemical gradient generated across mitochondrial inner membrane by the ETC [50]. Mitochondrial membrane potential supplies proton-motive force to promote translocation of proton from mitochondrial matrix to the intermembrane space, which is necessary for ATP synthesis. In addition to being the power center of the cell, mitochondria also generates reactive oxygen species (ROS), which originate from the electron leak from ETC. It has been well known that damage of mitochondria presented typical alterations

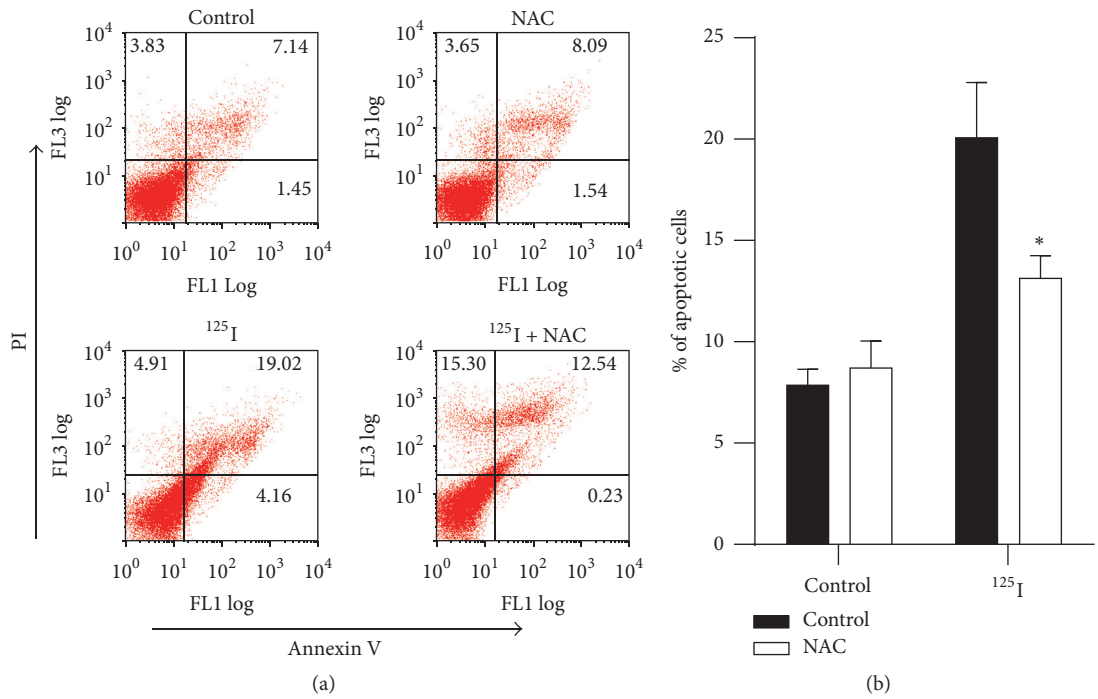


FIGURE 8: NAC decrease the proportion of apoptosis induced by $^{125}$I seeds radiation. HCT116 cells were incubated with and without 5 mmol of NAC for 4 hours and then either mock exposed or exposed to 2 Gy of $^{125}$I seeds radiation. (a) Annexin V and PI double staining was used to detect the distribution of cells after the indicated treatments. The typical examples of flow cytometry are shown. (b) Quantitative analysis of the percentage of apoptosis ($PI^-$/Annexin $V^+$ and $PI^+$/Annexin $V^+$ cell population). The values are the means ± SD of three independent experiments. ∗ indicates a significant difference ($p \leq 0.05$) as compared to the control group.

in mitochondrial morphology accompanied by biochemical changes, such as decreased ATP, decreased mitochondrial membrane potential, and increased mitochondrial ROS [51]. We therefore measured mitochondrial parameters after exposure to 2 Gy of $^{125}$I seeds radiation. We demonstrated that $^{125}$I seeds radiation had a significant impact on mitochondrial function, causing cell-specific disruption of mitochondrial membrane potential, reduction in the production of ATP, and accumulation of both cellular and mitochondrial ROS (Figure 6). These results indicated that oxidative stress induced by $^{125}$I seeds radiation increased the concentration of reactive oxygen species and led to mitochondrial dysfunction by inhibiting mitochondrial respiration.

The sources of mitochondrial ROS overproduction are the electron leak from mitochondrial ETC. Complexes I and III of ETC are regarded as major sites of mitochondrial ROS producers [52]. Specific inhibitors can inhibit complexes I and III of ETC and induce the leak of electrons, which results in a higher rate of mitochondrial ROS [53]. We used ROS inhibitor or mitochondrial ROS enhancer to influence the level of mitochondrial ROS and investigate the role of mitochondrial ROS in mitophagy induced by $^{125}$I seeds radiation. As a ROS scavenger NAC can block intracellular and mitochondrial ROS induced by $^{125}$I seeds radiation. After treatment with NAC, LC3-II accumulation induced by $^{125}$I seeds radiation decreased (Figures 7(a)–7(e)). Antimycin A, which blocks electron flow at complex III, is well known for increasing mitochondrial ROS and further increases mitophagy induced by $^{125}$I seeds radiation [54]. Diphenyleneiodonium (DPI) acting as a cellular superoxide production inhibitor by inhibition of mitochondrial respiratory chain complex I NADH reductase resulted in the potential to increase the production of mitochondrial superoxide [55]. As shown in Figures 7(f)–7(h), the treatment of DPI and Antimycin A raised mitochondrial ROS and further raised mitophagy induced by $^{125}$I seeds radiation. These results suggested that the accumulation of mitochondrial ROS induced by $^{125}$I seeds radiation is an important intracellular factor that contributes to trigger mitophagy.

ROS can damage cellular components and activate numerous signaling pathways to induce mitophagy. HIF-1$\alpha$ activated by ROS is an important signaling protein that regulates mitophagy by transcriptional regulation of its target genes BNIP3 and its homologue NIX [17, 56]. ROS upregulates HIF-1$\alpha$ transcription by activating nonhypoxic factors in a redox-sensitive manner [57]. Therefore, we investigated whether the accumulation of ROS induced by $^{125}$I seeds radiation activated HIF-1$\alpha$ and its target genes BNIP3 and NIX and thus triggered mitophagy. We demonstrated that $^{125}$I seeds radiation elevated mitochondrial ROS and the expression of HIF-1$\alpha$ and its target genes BNIP3 and NIX (Figures 9(a)–9(c)). It was noteworthy that inhibition of ROS by NAC not only reduced the ROS level but also the expression of HIF-1$\alpha$ and its target genes BNIP3 and NIX (Figures 9(d)–9(f)). Furthermore, mitochondrial electron transport chain inhibitors (DPI and Antimycin A) raised the accumulation

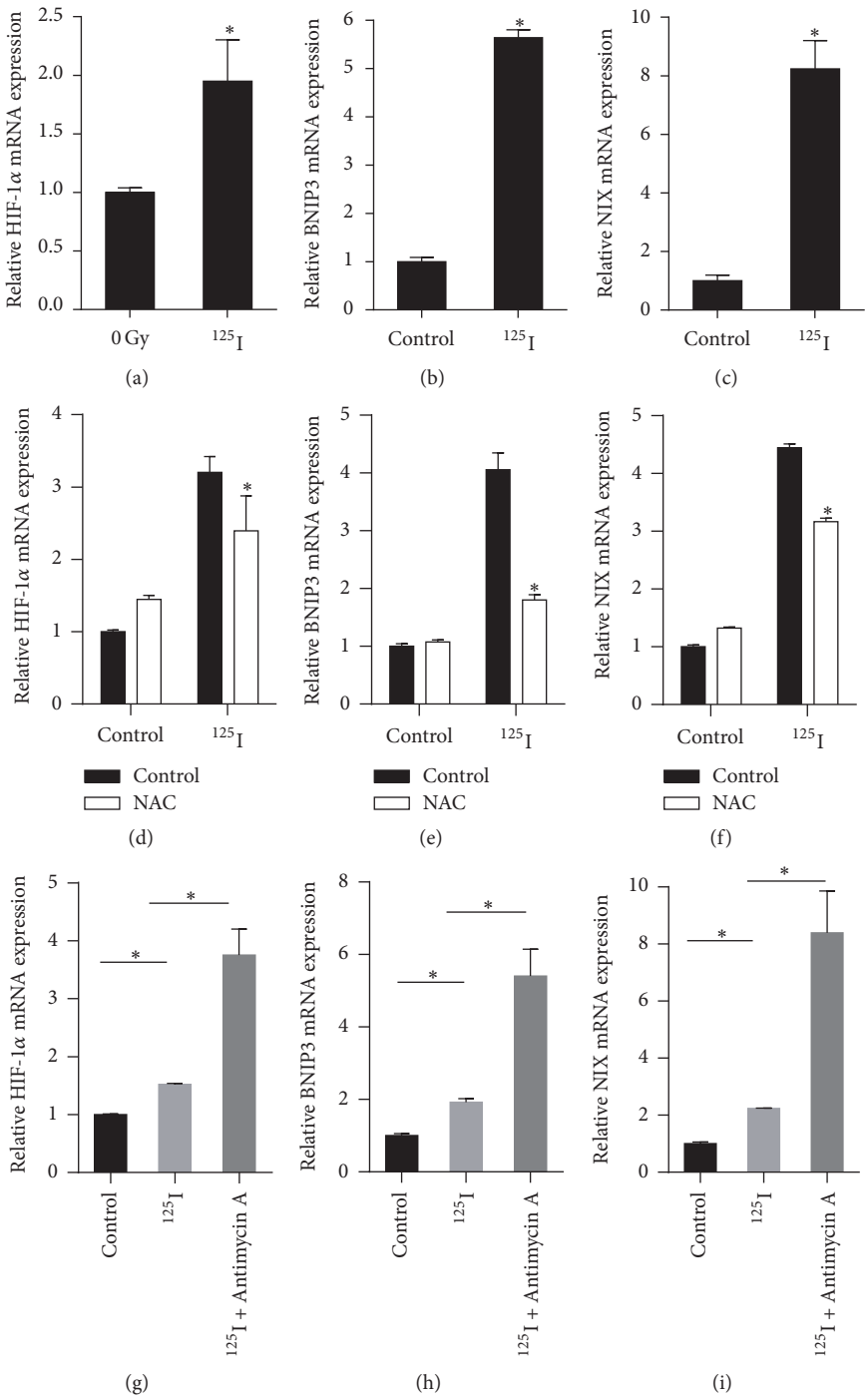


Figure 9: Mitochondrial ROS induced by $^{125}$I seeds irradiation is critical for the expression of HIF-1$\alpha$ and its target gene. (a–c) HCT116 cells were exposed to 2 Gy of $^{125}$I seeds radiation. Real-time PCR was performed to detect the expression of HIF-1$\alpha$ (a), BNIP3 (b), and NIX (c). (d–f) HCT116 cells were pretreated with and without 5 mM of NAC for 4 hours and then either mock exposed or exposed to 2 Gy of $^{125}$I seeds radiation. The level of mRNA of HIF-1$\alpha$ (d), BNIP3 (e), and NIX (f) was detected by real-time PCR after treatment. (g–h) The irradiated HCT116 cells were treated with or without 50 uM of Antimycin A for 18 hours before harvest. The level of mRNA of HIF-1$\alpha$ (g), BNIP3 (h), and NIX (i) was detected by real-time PCR after treatment. $*$ indicates a significant difference ($p \leq 0.05$) between NAC treated and untreated cells.

of mitochondrial ROS level and the expression of HIF-1$\alpha$ and its target genes BNIP3 and NIX (Figures 9(g)–9(i)). These results suggested that mitochondrial ROS induced by $^{125}$I seeds radiation upregulated the expression of HIF-1$\alpha$ and its target genes BNIP3 and NIX to trigger mitophagy.

BNIP3 and NIX can interact with BCL2 and BCL-XL to play a proapoptotic role. Deregulation of BNIP3 or NIX expression is associated with apoptosis [58]. We therefore hypothesized that ROS accumulation induced by $^{125}$I seeds radiation might play a critical role in cell fate determination. To test this theory, we used NAC to explore how ROS accumulation affects cell fate. Strikingly, NAC inhibited the percentage of apoptosis induced by $^{125}$I seeds radiation (Figures 8(a) and 8(b)), suggesting that mitochondrial ROS accumulation induced by $^{125}$I seeds radiation not only triggered mitophagy through upregulation of the expression of HIF-1$\alpha$ and its target genes but was also involved in the cellular decision of apoptosis.

## 5. Conclusions

Our results show that the high level of mitochondrial ROS generated by $^{125}$I seeds radiation induced mitochondrial damage upregulates the expression of HIF-1$\alpha$ and its target genes BNIP3 and NIX and triggers mitophagy. Mitophagy serves to reduce oxidative damage and ROS levels through the removal of damaged mitochondria, thus protecting HCT116 cells from apoptosis.

## Competing Interests

All authors of the paper have no financial and personal relationships with other people or organizations that could inappropriately influence this work.

## Authors' Contributions

Junjie Wang and Yong Zhao designed the study. Lelin Hu carried out the molecular biology experiment. Hao Wang and Li Huang participated in the statistical analysis. Lelin Hu wrote the manuscript. Junjie Wang and Yong Zhao revised the manuscript. All authors read and approved the final manuscript.

## Acknowledgments

The authors thank Associate Professor Guopeng Wang, who worked in School of life Sciences, Peking University, for technical assistance and giving advice regarding transmission electron microscopy technology for this study. The authors thank Professor Xiaojuan Du, who worked in Peking University Health Science Center, for providing the HCT116 cell line. This work was supported by grants from the National Natural Science Foundation for Young Scholars (81402519, Hao Wang).

## References

[1] J. J. Wang, H. S. Yuan, J. N. Li, W. J. Jiang, Y. L. Jiang, and S. Q. Tian, "Interstitial permanent implantation of 125I seeds as salvage therapy for re-recurrent rectal carcinoma," *International Journal of Colorectal Disease*, vol. 24, no. 4, pp. 391–399, 2009.

[2] J. Wang, Y. Jiang, J. Li, S. Tian, W. Ran, and D. Xiu, "Intraoperative ultrasound-guided iodine-125 seed implantation for unresectable pancreatic carcinoma," *Journal of Experimental and Clinical Cancer Research*, vol. 28, no. 1, article 88, 2009.

[3] J. Li, J. Wang, N. Meng et al., "Image-guided percutaneous $^{125}$I seed implantation as a salvage treatment for recurrent soft tissue sarcomas after surgery and radiotherapy," *Cancer Biotherapy and Radiopharmaceuticals*, vol. 26, no. 1, pp. 113–120, 2011.

[4] L. Zhu, Y. Jiang, J. Wang et al., "An investigation of $^{125}$I seed permanent implantation for recurrent carcinoma in the head and neck after surgery and external beam radiotherapy," *World Journal of Surgical Oncology*, vol. 11, article 60, 2013.

[5] L. Yao, J. Wang, Y. Jiang et al., "Permanent interstitial $^{125}$I seed implantation as a salvage therapy for pediatric recurrent or metastatic soft tissue sarcoma after multidisciplinary treatment," *World Journal of Surgical Oncology*, vol. 13, no. 1, article 335, 2015.

[6] L. Yao, Y. Jiang, P. Jiang et al., "CT-guided permanent $^{125}$I seed interstitial brachytherapy for recurrent retroperitoneal lymph node metastases after external beam radiotherapy," *Brachytherapy*, vol. 14, no. 5, pp. 662–669, 2015.

[7] Q. Cao, H. Wang, N. Meng et al., "CT-guidance interstitial $^{125}$Iodine seed brachytherapy as a salvage therapy for recurrent spinal primary tumors," *Radiation Oncology*, vol. 9, no. 1, article 301, 2014.

[8] Y. Tian, Q. Xie, Y. Tian et al., "Radioactive $^{125}$I seed inhibits the cell growth, migration, and invasion of nasopharyngeal carcinoma by triggering DNA damage and inactivating VEGF-A/ERK signaling," *PLoS ONE*, vol. 8, no. 9, Article ID e74038, 2013.

[9] J. Liu, H. Wang, A. Qu, J. Li, Y. Zhao, and J. Wang, "Combined effects of C225 and 125-iodine seed radiation on colorectal cancer cells," *Radiation Oncology*, vol. 8, no. 1, article 219, 2013.

[10] A. Qu, H. Wang, J. Li et al., "Biological effects of $^{125}$I seeds radiation on A549 lung cancer cells: G2/M arrest and enhanced cell death," *Cancer Investigation*, vol. 32, no. 6, pp. 209–217, 2014.

[11] B. Zhang, M. M. Davidson, H. Zhou, C. Wang, W. F. Walker, and T. K. Hei, "Cytoplasmic irradiation results in mitochondrial dysfunction and DRP1-dependent mitochondrial fission," *Cancer Research*, vol. 73, no. 22, pp. 6700–6710, 2013.

[12] W. W.-Y. Kam and R. B. Banati, "Effects of ionizing radiation on mitochondria," *Free Radical Biology and Medicine*, vol. 65, pp. 607–619, 2013.

[13] M. Saraste, "Oxidative phosphorylation at the fin de siecle," *Science*, vol. 283, no. 5407, pp. 1488–1493, 1999.

[14] P. A. Ney, "Mitochondrial autophagy: origins, significance, and role of BNIP3 and NIX," *Biochimica et Biophysica Acta—Molecular Cell Research*, vol. 1853, no. 10, pp. 2775–2783, 2015.

[15] B. Cheng, A. Xu, M. Qiao et al., "BECN1s, a short splice variant of BECN1, functions in mitophagy," *Autophagy*, vol. 11, no. 11, pp. 2048–2056, 2015.

[16] L. Liu, K. Sakakibara, Q. Chen, and K. Okamoto, "Receptor-mediated mitophagy in yeast and mammalian systems," *Cell Research*, vol. 24, no. 7, pp. 787–795, 2014.

[17] A. H. Chourasia, K. Tracy, C. Frankenberger et al., "Mitophagy defects arising from BNip3 loss promote mammary tumor

progression to metastasis," *EMBO Reports*, vol. 16, no. 9, pp. 1145–1163, 2015.

[18] A. Viale, P. Pettazzoni, C. A. Lyssiotis et al., "Oncogene ablation-resistant pancreatic cancer cells depend on mitochondrial function," *Nature*, vol. 514, no. 7524, pp. 628–632, 2014.

[19] H. Wu, D. Xue, G. Chen et al., "The BCL2L1 and PGAM5 axis defines hypoxia-induced receptor-mediated mitophagy," *Autophagy*, vol. 10, no. 10, pp. 1712–1725, 2014.

[20] T. E. O'Sullivan, L. R. Johnson, H. H. Kang, and J. C. Sun, "BNIP3- and BNIP3L-mediated mitophagy promotes the generation of natural killer cell memory," *Immunity*, vol. 43, no. 2, pp. 331–342, 2015.

[21] N. Wilfinger, S. Austin, B. Scheiber-Mojdekhar et al., "Novel p53-dependent anticancer strategy by targeting iron signaling and BNIP3L-induced mitophagy," *Oncotarget*, vol. 7, no. 2, pp. 1242–1261, 2016.

[22] D. R. Green and B. Levine, "To be or not to be? How selective autophagy and cell death govern cell fate," *Cell*, vol. 157, no. 1, pp. 65–75, 2014.

[23] N. M. Mazure and J. Pouysségur, "Hypoxia-induced autophagy: cell death or cell survival?" *Current Opinion in Cell Biology*, vol. 22, no. 2, pp. 177–180, 2010.

[24] E. I. Braicu, H. Luketina, R. Richter et al., "HIF1$\alpha$ is an independent prognostic factor for overall survival in advanced primary epithelial ovarian cancer—a study of the OVCAD consortium," *OncoTargets and Therapy*, vol. 7, pp. 1563–1569, 2014.

[25] L. Li, J. Tan, Y. Miao, P. Lei, and Q. Zhang, "ROS and autophagy: interactions and molecular regulatory mechanisms," *Cellular and Molecular Neurobiology*, vol. 35, no. 5, pp. 615–621, 2015.

[26] H.-Q. Zhuang, J.-J. Wang, A.-Y. Liao, J.-D. Wang, and Y. Zhao, "The biological effect of $^{125}$I seed continuous low dose rate irradiation in CL187 cells," *Journal of Experimental and Clinical Cancer Research*, vol. 28, no. 1, article 12, 2009.

[27] H. Wang, J. Li, A. Qu, J. Liu, Y. Zhao, and J. Wang, "The different biological effects of single, fractionated and continuous low dose rate irradiation on CL187 colorectal cancer cells," *Radiation Oncology*, vol. 8, no. 1, article 196, 2013.

[28] T. Yan, Y. Seo, and T. J. Kinsella, "Differential cellular responses to prolonged LDR-IR in MLH1-proficient and MLH1-deficient colorectal cancer HCT116 cells," *Clinical Cancer Research*, vol. 15, no. 22, pp. 6912–6920, 2009.

[29] L. Zhu, T. Yang, L. Li et al., "TSC1 controls macrophage polarization to prevent inflammatory disease," *Nature Communications*, vol. 5, Article ID 4696, 2014.

[30] L. Guo, H. Yu, W. Gu et al., "Autophagy negatively regulates transmissible gastroenteritis virus replication," *Scientific Reports*, vol. 6, Article ID 23864, 2016.

[31] L. Hu, H. Wang, L. Huang, Y. Zhao, and J. Wang, "Crosstalk between autophagy and intracellular radiation response (Review)," *International Journal of Oncology*, vol. 49, no. 6, pp. 2217–2226, 2016.

[32] Y. Jiang, J. Lee, J. H. Lee et al., "The arginylation branch of the N-end rule pathway positively regulates cellular autophagic flux and clearance of proteotoxic proteins," *Autophagy*, vol. 12, no. 11, pp. 2197–2212, 2016.

[33] M. J. Lee, J. H. Lee, and D. C. Rubinsztein, "Tau degradation: the ubiquitin-proteasome system versus the autophagy-lysosome system," *Progress in Neurobiology*, vol. 105, pp. 49–59, 2013.

[34] D. J. Klionsky, H. Abdalla, H. Abeliovich et al., "Guidelines for the use and interpretation of assays for monitoring autophagy," *Autophagy*, vol. 8, no. 4, pp. 445–544, 2012.

[35] S. Banerjee, N. Aykin-Burns, K. J. Krager et al., "Loss of C/EBP$\delta$ enhances IR-induced cell death by promoting oxidative stress and mitochondrial dysfunction," *Free Radical Biology and Medicine*, vol. 99, pp. 296–307, 2016.

[36] X. Wang, M. Yan, L. Zhao et al., "Low-dose methylmercury-induced apoptosis and mitochondrial DNA mutation in human embryonic neural progenitor cells," *Oxidative Medicine and Cellular Longevity*, vol. 2016, Article ID 5137042, 10 pages, 2016.

[37] M. B. E. Schaaf, B. Jutten, T. G. Keulers et al., "Canonical autophagy does not contribute to cellular radioresistance," *Radiotherapy and Oncology*, vol. 114, no. 3, pp. 406–412, 2015.

[38] H. Weidberg, E. Shvets, and Z. Elazar, "Biogenesis and cargo selectivity of autophagosomes," *Annual Review of Biochemistry*, vol. 80, pp. 125–156, 2011.

[39] B. B. Chandrika, C. Yang, Y. Ou et al., "Endoplasmic reticulum stress-induced autophagy provides cytoprotection from chemical hypoxia and oxidant injury and ameliorates renal ischemia-reperfusion injury," *PLoS ONE*, vol. 10, no. 10, Article ID e0140025, 2015.

[40] J. J. Jaboin, E. T. Shinohara, L. Moretti, E. S. Yang, J. M. Kaminski, and B. Lu, "The role of mTOR inhibition in augmenting radiation induced autophagy," *Technology in Cancer Research and Treatment*, vol. 6, no. 5, pp. 443–447, 2007.

[41] Q. Sun, T. Liu, Y. Yuan et al., "MiR-200c inhibits autophagy and enhances radiosensitivity in breast cancer cells by targeting UBQLN1," *International Journal of Cancer*, vol. 136, no. 5, pp. 1003–1012, 2015.

[42] N. Chen, L. Wu, H. Yuan, and J. Wang, "ROS/autophagy/Nrf2 pathway mediated low-dose radiation induced radio-resistance in human lung adenocarcinoma A549 cell," *International Journal of Biological Sciences*, vol. 11, no. 7, pp. 833–844, 2015.

[43] K. W. Kim, L. Moretti, L. R. Mitchell, K. J. Dae, and B. Lu, "Combined Bcl-2/mammalian target of rapamycin inhibition leads to enhanced radiosensitization via induction of apoptosis and autophagy in non-small cell lung tumor xenograft model," *Clinical Cancer Research*, vol. 15, no. 19, pp. 6096–6105, 2009.

[44] A. Apel, I. Herr, H. Schwarz, H. P. Rodemann, and A. Mayer, "Blocked autophagy sensitizes resistant carcinoma cells to radiation therapy," *Cancer Research*, vol. 68, no. 5, pp. 1485–1494, 2008.

[45] M. Chaurasia, A. N. Bhatt, A. Das, B. S. Dwarakanath, and K. Sharma, "Radiation-induced autophagy: mechanisms and consequences," *Free Radical Research*, vol. 50, no. 3, pp. 273–290, 2016.

[46] G. Kroemer, G. Mariño, and B. Levine, "Autophagy and the integrated stress response," *Molecular Cell*, vol. 40, no. 2, pp. 280–293, 2010.

[47] Y. Kabeya, N. Mizushima, T. Ueno et al., "LC3, a mammalian homologue of yeast Apg8p, is localized in autophagosome membranes after processing," *The EMBO Journal*, vol. 19, no. 21, pp. 5720–5728, 2000.

[48] C. De Duve and R. Wattiaux, "Functions of lysosomes," *Annual Review of Physiology*, vol. 28, pp. 435–492, 1966.

[49] R. J. Youle and D. P. Narendra, "Mechanisms of mitophagy," *Nature Reviews Molecular Cell Biology*, vol. 12, no. 1, pp. 9–14, 2011.

[50] S. Hekimi, Y. Wang, and A. Noë, "Mitochondrial ROS and the effectors of the intrinsic apoptotic pathway in aging cells: the discerning killers!," *Frontiers in Genetics*, vol. 7, article 161, 2016.

[51] L. Galam, A. Failla, R. Soundararajan, R. F. Lockey, and N. Kolliputi, "4-Hydroxynonenal regulates mitochondrial function in

human small airway epithelial cells," *Oncotarget*, vol. 6, no. 39, pp. 41508–41521, 2015.

[52] D. Babu, G. Leclercq, V. Goossens et al., "Mitochondria and NADPH oxidases are the major sources of TNF-$\alpha$/cycloheximide-induced oxidative stress in murine intestinal epithelial MODE-K cells," *Cellular Signalling*, vol. 27, no. 6, pp. 1141–1158, 2015.

[53] P. R. Angelova and A. Y. Abramov, "Functional role of mitochondrial reactive oxygen species in physiology," *Free Radical Biology and Medicine*, vol. 100, pp. 81–85, 2016.

[54] D. Rakhmatullina, A. Ponomareva, N. Gazizova, and F. Minibayeva, "Mitochondrial morphology and dynamics in *Triticum aestivum* roots in response to rotenone and antimycin A," *Protoplasma*, vol. 253, no. 5, pp. 1299–1308, 2016.

[55] N. Li, K. Ragheb, G. Lawler et al., "DPI induces mitochondrial superoxide-mediated apoptosis," *Free Radical Biology and Medicine*, vol. 34, no. 4, pp. 465–477, 2003.

[56] S. Movafagh, S. Crook, and K. Vo, "Regulation of hypoxia-inducible factor-1a by reactive oxygen species: new developments in an old debate," *Journal of Cellular Biochemistry*, vol. 116, no. 5, pp. 696–703, 2015.

[57] S. Bonello, C. Zahringer, R. S. BelAiba et al., "Reactive oxygen species activate the HIF-1$\alpha$ promoter via a functional NF$\kappa$B site," *Arteriosclerosis, Thrombosis, and Vascular Biology*, vol. 27, no. 4, pp. 755–761, 2007.

[58] J. Zhang and P. A. Ney, "Role of BNIP3 and NIX in cell death, autophagy, and mitophagy," *Cell Death and Differentiation*, vol. 16, no. 7, pp. 939–946, 2009.